Proceedings of the 2005 IEEE
Engineering in Medicine and Biology 27th Annual Conference
Shanghai, China, September 1-4, 2005

Optimization of Off-null Ellipsometry for Optical Biosensor Applications

Yanyan Chen[a,b], Yonghong Meng[a,b], and Gang Jin[a]*
[a] Institute of Mechanics, Chinese Academy of Sciences, #15, Bei-si-huan west Rd., Beijing 100080, P.R. China
[b] Graduate School of Chinese Academy of Sciences, #19, Yu-quan Rd, Shi-jing-shan District, Beijing 100039, P.R. China
*Corresponding author: Tel./Fax.: +86-10-62631816, E-mail: gajin@imech.ac.cn

Abstract- **The optimization of off-null ellipsometry is described with emphasis on the improvement of resolution for visualizing biomolecule layers. For optical biosensor with layer thickness below 6.5 nm, a numerical simulation for the dependence of resolution on the azimuth settings of polarizer and analyzer is presented first. For comparison, three different resolutions are given at three azimuth settings which are near null and far away from null condition, respectively. Furthermore, the square or linear approximation relationship between the intensity and the layer thickness are also given at these settings. The difference among their accuracy is up to 100 times or so. Experimental results of the biosensor sample verify the optimization.**

Keywords-Biosensor, off-null ellipsometry, optimization

I. INTRODUCTION

The biosensor based on imaging ellipsometry for visualization of biomolecular interactions was reported in 1995 [1, 2]. The basic principle is that each reactant as a ligand is immobilized to a surface to form a monolayer as a bioprobe with its bioactivity. The other reactant as the analyte (or receptor) exists in a solution. The bioprobe is exposed to the solution containing analyte. When the analyte in the solution interacts with its corresponding ligand on the bioprobe and assembles into complex upon their affinity. The molecule surface concentration on the surface where the interaction takes place becomes higher than before exposure to the analyte solution. A significant increase of the layer thickness (surface concentration) indicates that the solution contained receptor against the ligand on the surface. The biosensor has become an automatic analysis technique for protein detection with merits of label-free, multi-protein analysis, and real-time analysis for protein interaction process, etc [3]. As the visualization method for biosensor, the imaging ellipsometry performing sampling technique with off-null ellipsometry may visualize the spatial variations in protein layers with distinct graph and explain results with qualitative and quantitative analysis. Its intensity measurement provides a faster sampling speed and a measurement for a large field of view of a sample surface at the same time. Hence, multiple analytes could be detected simultaneously. The high stability and the high sensitivity to reflection make it suitable to measure thin transparent organic layers. However, for such layers on a solid substrate, the relative amplitude and phase changes between incident and reflection rely on accurate intensity measurement. In order to perform the biosensor technique with the highest resolution, the optimization of off-null ellipsometry must be taken into account.

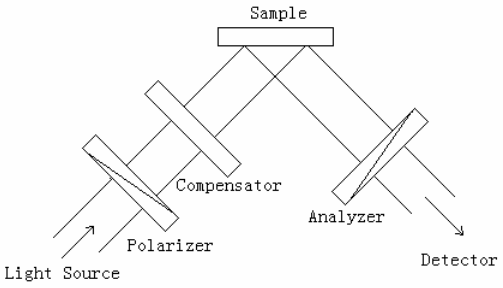

Fig. 1. Schematic diagram of an off-null PCSA ellipsometer.

II. THEORETICAL AND EXPERIMENTAL ANALYSIS

A. Theoretical Analysis

Fig.1 shows the schematic diagram of the basic experimental set-up, which is based on a PCSA configuration [4] that consists of a polarizer, a compensator, a sample, and an analyzer (P, C and A denote their azimuth angles, respectively).

By applying a Jones vector and matrix approach using the notation convention of R.M.A. Azzam and N.M. Bashara, a theoretical expression for the detected intensity (denoted by I) related to P, C, and A as well as the sample properties can be expressed as [4]

$$\begin{aligned} I &= K(|R_s|^2/2)\{[1+\cos 2C\cos 2(P-C)]\cos^2 A\tan^2\psi \\ &\quad +[1-\cos 2C\cos 2(P-C)]\sin^2 A \\ &\quad +[\sin 2C\cos 2(P-C)\cos\Delta \\ &\quad -\sin 2(P-C)\sin\Delta]\sin 2A\tan\psi\} \\ &= KI_0 \end{aligned} \quad , (1)$$

where K is a constant. The amplitude $\tan\psi$ and phase Δ are the basic measurement parameters in ellipsometry, and are defined by the complex-valued ratio

$$\rho = R_p/R_s = \tan\psi e^{i\Delta} \quad , \qquad (2)$$

where R_p and R_s are the complex reflection coefficients of

light polarized parallel (*p* direction) and perpendicular (*s* direction), respectively, to the plane of incidence.

Eq. (1) is based on the assumption that the compensator is ideal with the slow-to-fast relative complex-amplitude transmittance $\rho_c = -i = -\sqrt{-1}$. When the compensator is fixed at 45º, the intensity I_0 is a function of the properties of the sample and the azimuth angles of the polarizer and the analyzer. Here, the thickness of a biomolecule layer is of main interest. The resolution for layer thickness denoted by r is defined as $r=\delta I_0/\delta d$, where δI_0 indicates the intensity changes relative to thickness difference δd between layers. For two known thin layers, their difference in intensity δI_0 depending on P and A can be obtained by Eq.(1). In this way, proper settings can be chosen for high resolution.

Usually the refractive index of saturated protein layers in visible light region is in the range of 1.4-1.5 [5], and the relative variation of layer thickness is interested, but not the absolute value of the thickness, so it's simplified that the refractive indices of protein layers are supposed the same. In addition, the optical properties of SiO_2 and protein are so similar that they are supposed the same. Therefore, the sample under investigation is air/SiO_2/silicon substrate with the layer thickness d in the range of 1.8-6.5nm. N_0=1.0, N_1=1.457, and N_2=3.858-i0.018 are the refractive indices of ambient, layer and substrate, respectively, at the wavelength of 630nm. For the numerical simulation, two SiO_2 layers with thickness 2nm and 3nm, respectively, on silicon substrate as a sample is considered at the angle of incidence 73.8º. The simulated intensity change δI_0 depending on P and A is represented by a contour map in Fig.2.

Obviously, the proper azimuth settings with which to obtain different resolution r can be chosen by this contour map. Once the azimuth angles are fixed, the relationship between I_0 and d in the thickness range of sample is fixed, which may be simplified by a first order approximation, or a high order approximation with a higher precision. The simplified relationship is important to establish calibration curve for the quantitative measurement of the biosensor.

For comparison, three settings are given to show different

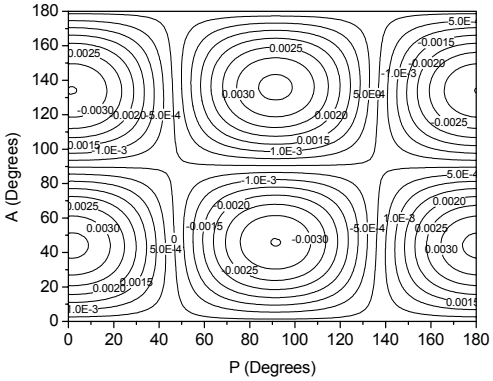

Fig. 2. Simulated contour map of δI_0, related to P and A varied from 0 to180º, respectively, with the following parameters: $|R_s|^2$=0.741; ψ=3.70º, Δ=160.35º, which are corresponding to a SiO_2 layer with d=2 nm; and ψ=3.89º, Δ=152.58º, which are corresponding to another SiO_2 layer with d=3 nm.

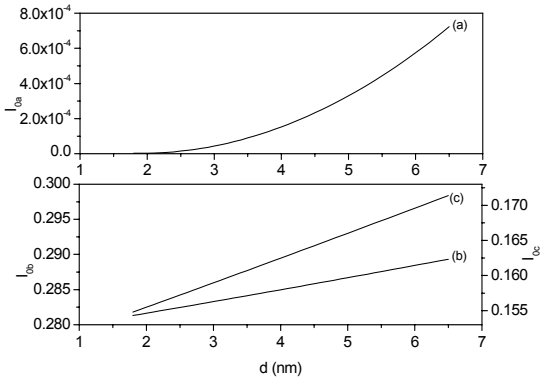

Fig. 3. The intensity versus the thicknesses of samples in the range of 1.8-6.5nm at three different settings, which correspond to (a) a null settings at where A=3.83º, P=54.10º, the curve is fitted to $I_{0a}=3.4\times10^{-5}d^2-1.29\times10^{-4}d+1.25\times10^{-4}$, (b) the better settings at where A=62.82º, P=28.86º, the curve is fitted to $I_{0b}=1.71\times10^{-3}d+0.28$ and (c) the optimal settings at where A=44.67º, P=0.19º, the curve is fitted to $I_{0c}=3.63\times10^{-3}d+0.18$.

resolutions and their approximate relationships between I_0 and d by Eq.(1). The azimuth angles that reduced the detected light flux to minimal at somewhere on a sample or the bare substrate under investigation are defined as null settings, and off-null settings otherwise. Now that the azimuth angles in most works [1-3,7-9] are fixed at or close to the null settings, it is necessary to consider the null condition in this work. The null settings chosen correspond to the azimuth angles that fulfill the null conditions on the SiO_2 layer with d=1.8nm. The better settings and the optimal settings chosen are all off-null settings. Fig.3 shows how the intensity depends on the thickness of samples in the range of 1.8-6.5nm at three settings. These curves demonstrate clearly the different resolution at three settings. In Table 1, the detailed settings and the resolutions are given, as well as the relationship between I_0 and d determined by simulating these curves numerically according to approximation analysis within reasonable relative error levels. Curve (a) is also considered by a first order approximation, which cause the corresponding relative error > 10%, and not to be accepted. Then, second order approximation is considered and the square relationship with relative error >1% is obtained.

Clearly, it can be seen that the lowest resolution r_a is obtained near the null settings, as well as the nonlinear relationship between I_0 and d with the largest error. On the contrary, curve (c) at optimal settings is corresponding to a simple linear relationship with the least error and the highest resolution r_c. The resolution is also found to increase more than 20 times and the relative error is reduced to about 1/100 for the optimal settings compared with the null settings. The error level and relationship are almost the same, but resolution is decreased 50% for the better settings

Table 1. Azimuth settings, relationship, error and resolution of three different settings are shown corresponding to Fig.3.

	Azimuth Angle Setting(°)				
Type	P	A	relationship	error	r(×10^{-3})
a	54.10	3.83	square	>1%	0.15
b	28.86	62.82	linear	0.02%	1.71
c	0.19	44.67	linear	0.03%	3.63

compared with the optimized settings.

B. Experimental Analysis

For verifying above theoretical analysis, some experiments on samples of SiO_2 layers/Si substrate are performed with a PCSA experimental system, in which a charge-coupled-device (CCD) camera is used as a detector and a 75W xenon arc lamp and a collimating system are used as a light source to provide an expanded parallel probe beam, which make intensity fit to the linear dynamic range of the detector. The polarizer and the analyzer are dichroic sheet polarizer with extinction ratio 10^{-4}, and a mica retardation of quarter-wave plate is used as the compensator. Finally, the results are stored as the images in grayscale format (8 bit, 256 gray scales) for further evaluation by an image processing program. CCD camera is a Sony XC-ST30 CCD B/W video camera, and it has been proved the dynamic range of the detector is linear when the gray scale is among 15-230 in the off-null ellipsometry.

Fig.5 shows the experimental results which are obtained at the azimuth angle settings mentioned above. The difference in gray scales between 6.5 nm and 1.8 nm SiO_2 layers is below 0.5 at the null settings, which is so difficult to recognize different layers in samples that the experimental result does not shown in Fig.5. Curve (b) and (c) are obtained at the other two settings, and I_b=1.16d+216.51 and I_c=2.34d+135.99 are obtained by fitting two curves, respectively, with the relative errors all within ± 0.2%. Note that the resolutions which are different from those in Table 1, the reason is K in Eq.(1) is not discussed in simulation analysis but included in experimental results. However, r_b=1.16/K is about a half r_c=2.34/K, which also proves the consistency of theory and experiment.

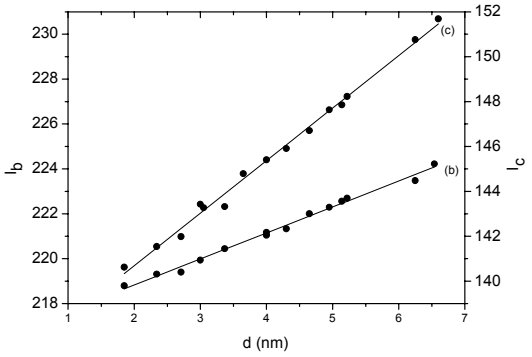

Fig. 5. Gray scales with respect to the thickness of SiO_2 layer in experiment. The dotted line is the experimental results; and the solid line is the fitting curve.

III. FURTHER OPTIMIZATION AND DISCUSSION

The thickness resolution can be improved by the adjustment of azimuth angles P and A. All of these are discussed without considering K in Eq.(1). For an experimental system, the resolution can be improved further by increasing the probe light intensity and considering the dynamic range of the detector since K is related to these [4]. Therefore, the final resolution for an experimental

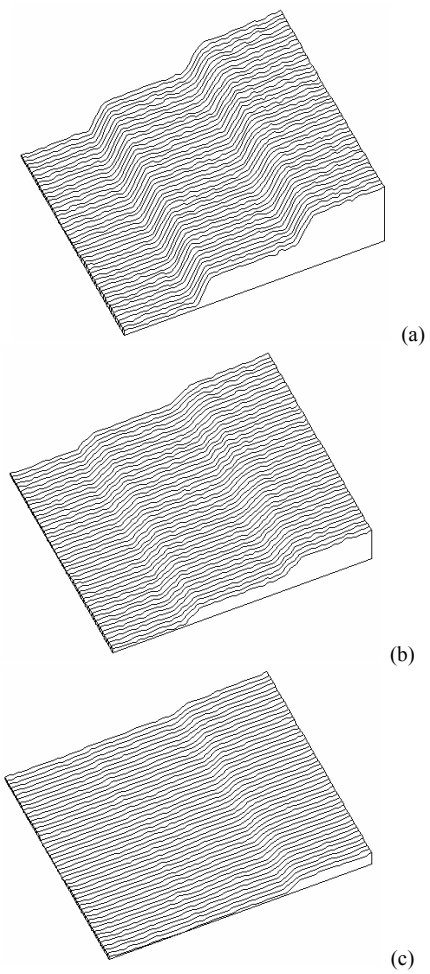

Fig. 6. Gray scales distribution on a silicon surface with a SiO_2 layer (left), h-IgG layer (middle), and h-IgG/anti-h-IgG complex layer (right) at (a) A=2.10º, P=8.70º, (b) A=0.10º, P=8.70º, and (c) A=3.83º, P=54.10º, respectively.

system is the product of K and r, which is limited by the dynamic range of detector in case of the intensity out of the range. The final resolution in Fig.5 (c) can be improved by increasing the probe light intensity to make the maximal gray scale up to 230. However, Fig.5 (b) is out of the dynamic range under the probe light intensity. Further increasing the probe light intensity, Fig.5 (c) is also out of the range and r must be decreased to make measurement in the dynamic range of the detector. Therefore, for a fixed high probe light intensity in our experimental system, the optimal resolution for biosensor system with thickness below 6.5nm is obtained at A=2.10º, P=8.70º. Fig.6 (a) shows the gray scale distribution of a stepped SiO_2 layer, human Immunoglobulin G (h-IgG) layer, and h-IgG/anti-h-IgG complex layer on the silicon substrate measured at the optimal settings. The thicknesses of three layers are 2.2 nm, 4.0 nm, and 5.9 nm, respectively, measured with conventional ellipsometer. The measurements are also performed at the other two settings to show different resolutions. Only changing the azimuth angle of analyzer to 0.1º on the experimental conditions as above, the result shown in Fig.6 (b) indicates the thickness

resolution is lower. Fig.6 (c) is gotten near the null settings (A=3.83º, P=54.10º) with the lowest resolution.

IV. CONCLUSION

An optimization of off-null ellipsometry for the biosensor sampling has been presented. The thickness resolution has been remarkably improved at the optimal setting. Moreover, the simplified approximation relationship between the intensity and layer thickness is the basis for the quantitative measurement of the biosensor system. All of these are helpful for applications of the biosensor.

ACKNOWLEDGEMENT

The National Natural Science Foundation of China and The Chinese Academy of Sciences are gratefully acknowledged for their supports.

REFERNCES

[1] G. Jin, P. Tengvall, I. Lundstršm and H. Arwin, "A Biosensor Concept Based on Imaging Ellipsometry for Visualization of Biomolecular Interactions," *Analytical Biochemistry*, vol.232, pp. 69-72, 1995.

[2] G. JIN, R. Jansson, and H. Arwin, "Imaging ellipsometry revisited: Developments for visualization of thin transparent layers on silicon substrates, "Rev. Sci. Instrum., vol.67, pp. 2930-2936, 1996.

[3] Z. H. Wang, G. Jin, "A label-free multisensing immunosensor based on Imaging Ellipsometry," *Analytical Chemistry*, vol.75, no. 22, pp. 6119-6123, 2003.

[4] R.M.A. Azzam and N.M. Bashara, *Ellipsometry and Polarized Light* (North-Holland, New York, 1977).

[5] H. Arwin, "Optical properties of thin layers of Bovine serum albumin, γ-globulin, and hemoglobin," *Applied Spectroscopy*, vol.40, no.3, pp.313-318, 1986.

[6] M. Stenberg, H. Nygren, "The use of the isoscope ellipsometer in the study of adsorbed proteins and biospecificbinding reactions," *J. Phys*. Vol.44, pp. 83–6, 1983.

[7] H. Arwin, S. Welin-Klintström, and R. Jansson, "Off-null ellipsometry revisited: basic consideration for measuring surface concentrations at solid/liquid interfaces," J. Colloid Interface Sci. 156, 377-382 (1993).

[8] G.L. Wang, H. Arwin, and R. Jansson, " Optimization of azimuth angle settings in polarizer-compensator-sample-analyzer off null ellipsometry," Appl. Opt. 42, 38-44 (2003).

[9] G.L. Wang, H. Arwin, and R. Jansson, " Optimization of off null ellipsometry in sensor applications," Appl. Opt. 43, 2000-2005 (2004)